1

Introduction to Internal Friction: Terms and Definitions

In this chapter, the reader is introduced into the terminology and nomenclature used in this book. The main subjects are defined and classified from the *phenomenological* point of view, and the related theoretical background and experimental techniques are reviewed briefly. The *microscopic* mechanisms, which are also included in the data collections as an important part of information, will then be introduced in Chaps. 2 and 3.

1.1 General Phenomenon

The phenomenon of *internal friction* – most generally defined as the dissipation of mechanical energy inside a gaseous, liquid or solid medium – is basically different from "friction" in the tribological sense, i.e., the resistance against the motion of two solid surfaces relative to each other ("external friction"). In a *solid material* exposed to a time-dependent load within the "elastic" deformation range – only this case is considered in this book – "internal friction" usually means energy dissipation connected with deviations from Hooke's law, as manifested by some stress–strain hysteresis in the case of cyclic loading. The corresponding energy absorption ΔW during one cycle, divided by the maximum elastic stored energy W during that cycle, defines the *specific damping capacity* $\Psi = \Delta W/W$, or the *loss factor* $\Delta W/2\pi W$, as the most general measures of internal friction, for which no further assumptions are required (but for most metallic materials this hysteresis is rather small, i.e., $\Psi \ll 1$). The reciprocal loss factor is also called the *quality factor* $Q = 2\pi W/\Delta W$ (Lazan 1968), so that "internal friction" or "damping" can generally be written as

$$Q^{-1} = \Delta W/2\pi W = \Psi/2\pi. \tag{1.1}$$

It should be mentioned, however, that for some of these terms deviating definitions exist, which will be discussed later in this introductory chapter. Also the nomenclature (usage of names and symbols) is not always clear,

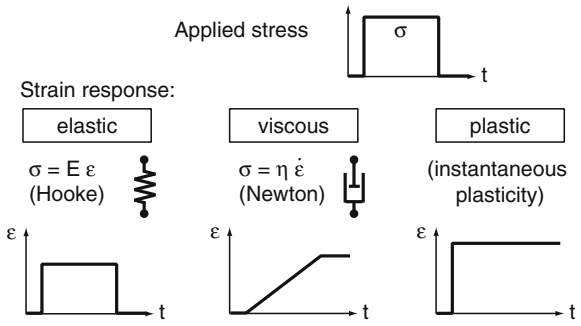

Fig. 1.1. Fundamental types of mechanical behaviour: response of strain $\varepsilon(t)$ to a constant stress of finite duration with abrupt loading and unloading

due to different traditions that have developed in the related scientific and technical disciplines. One example is the symbol η which is reserved here for the *viscosity* (see Fig. 1.1) according to its common use in physics, fluid mechanics and materials science (including glasses and polymers), but which has a second meaning as loss factor (or *loss coefficient*, Lazan 1968) in structural engineering and part of technical mechanics. In this book internal friction is – according to the tradition of materials science, physical metallurgy and solid-state physics from which *mechanical spectroscopy* has emerged – generally denoted as Q^{-1}.

1.2 Types of Mechanical Behaviour

Before characterising the types and sources of internal friction in more detail, we have to consider the phenomenology of mechanical behaviour; for this purpose, the use of mechanical (or rheological) models is very helpful. Elements of such models are deduced from fundamental types of mechanical behaviour of solids and liquids like those shown in Fig. 1.1; most important as linear elements are the spring and the dashpot which denote, respectively, an ideal (Hookean) *elastic* solid with stiffness or "modulus" E, and an ideal (Newtonian) *viscous* liquid with viscosity η (for non-linear models used to describe plasticity, see e.g. Palmov 1998, Fantozzi 2001). Combinations of springs and dashpots generally define viscoelastic behaviour (Palmov 1998), in particular *linear viscoelasticity* since the related constitutive equations are linear (for convenience we consider uniaxial deformation and scalar quantities, but the generalisation to the tensor form is straightforward).

Within this definition, the simplest case of linear viscoelasticity is represented by a Maxwell model, i.e., a spring and a dashpot in series. On the other hand, the respective parallel combination (Voigt–Kelvin model) is unrealistic because of infinite instantaneous stiffness. Whereas in principle any number of springs and dashpots can be combined, we have to distinguish

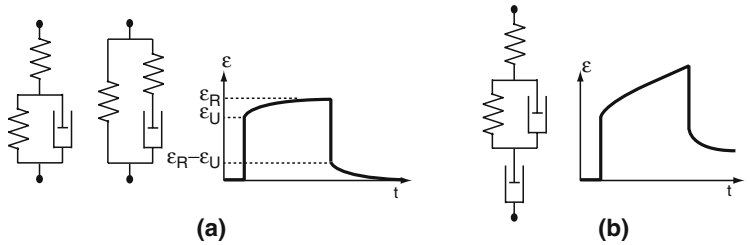

Fig. 1.2. Examples of viscoelastic mechanical models, with the same applied stress as in Fig. 1.1: (**a**) completely recoverable three-parameter models ("standard anelastic solid"); (**b**) partially recoverable four-parameter model

Table 1.1. Different existing terminologies for the distinction between recoverable and non-recoverable types of (linear) viscoelasticity

recoverable – non-recoverable	reference (example)
anelastic – viscoelastic	Nowick and Berry 1972
viscoelastic – viscoplastic	Fantozzi 2001, Rösler et al. 2003
viscoelastic – elastoviscous	Meyer and Guicking 1974
viscoelastic solid – viscoelastic liquid	Ferry 1970

between models with a continuous chain of springs resulting in a completely recoverable strain (or more precisely, a unique equilibrium relationship between stress and strain, Fig. 1.2a), and those with a single dashpot in series showing a permanent deformation after unloading (absence of a stress–strain equilibrium, Fig. 1.2b).

The terminology of this latter distinction (which can also be interpreted as a borderline between solids and liquids) is again not consistent throughout the scientific literature: a list of a few related definitions is given in Table 1.1. In the present book, a completely recoverable behaviour is named *anelastic* (Zener 1948, Krishtal et al. 1964, Lazan 1968, Nowick and Berry 1972, Lakes 1999) because this term appears to be the most clearly defined one. The corresponding approach to internal equilibrium, after an external perturbation, is known as *anelastic relaxation*. Non-recoverable components like in Fig. 1.2b may then be called "viscous" or "viscoplastic" (but are of minor importance in this book), whereas "viscoelasticity" may include both recoverable and non-recoverable behaviour (Lazan 1968, Ferry 1970, Palmov 1998, Lakes 1999).

1.3 Anelastic Relaxation

Anelastic relaxation, as the main source of internal friction considered in this book, is seen in Fig. 1.2a both as a saturating "creep" strain $\varepsilon(t)$ after loading, with "unrelaxed" and "relaxed" values ε_{U} and ε_{R}, and as a decaying "elastic

after-effect" after unloading, and may also be observed as stress relaxation in case of a constant applied strain. It is characterised by a *relaxation strength* $\Delta = (\varepsilon_\mathrm{R} - \varepsilon_\mathrm{U})/\varepsilon_\mathrm{U}$[1] which can be written in different ways – e.g. as $\Delta = (E_\mathrm{U} - E_\mathrm{R})/E_\mathrm{R}$ using a time-dependent modulus $E(t)$ defined for stress relaxation (generalised Hooke's law) – and by a distribution of *relaxation times* τ. In the simplest possible case, the so-called *standard anelastic solid* (Nowick and Berry 1972) or *standard linear solid* (Zener 1948, Fantozzi 2001) defined by the two equivalent three-parameter models in Fig. 1.2a, the time-dependent changes are of the form $\mathrm{e}^{-t/\tau}$ with a single relaxation time τ (either τ_σ for constant stress or τ_ε for constant strain, with $\tau_\sigma = \tau_\varepsilon = \tau$ for $\Delta \ll 1$).

More important in the context of this handbook, than this quasi-static behaviour of an anelastic solid, is that one under a *cyclic* applied stress or strain. In the linear theory of anelasticity (Nowick and Berry 1972), using the mathematically convenient complex notation (with complex quantities marked by an asterisk) for sinusoidally varying stress and strain,

$$\sigma^* = \sigma_0 \mathrm{e}^{\mathrm{i}\omega t} \quad \text{and} \quad \varepsilon^* = \varepsilon_0 \mathrm{e}^{\mathrm{i}(\omega t - \phi)} = (\varepsilon' - i\,\varepsilon'')\mathrm{e}^{\mathrm{i}\omega t}, \tag{1.2}$$

several dynamic response functions are defined as a function of the circular frequency ω like, for instance, a complex modulus

$$E^*(\omega) = \sigma^*/\varepsilon^* = E(\omega)\mathrm{e}^{\mathrm{i}\phi(\omega)} = E'(\omega) + iE''(\omega). \tag{1.3}$$

The real quantities $E(\omega)$, $E'(\omega)$ and $E''(\omega)$ are called *absolute dynamic modulus*, *storage modulus* and *loss modulus*, respectively; the phase lag ϕ between stress and strain is also known as the *loss angle*.[2] The real parts of (1.2) form the parametric equations of an ellipse as stress–strain hysteresis loop (not only in the anelastic case but generally for linear viscoelasticity), so that the calculation of the dissipated energy ΔW shows that in this case the *loss tangent* $\tan\phi$ is identical with the more generally defined loss factor introduced earlier (Fantozzi 2001):

$$Q^{-1} = \Delta W/2\pi W = \tan\phi = E''/E' = \varepsilon''/\varepsilon'. \tag{1.4}$$

The dynamic response functions of the standard anelastic solid are given by the well-known Debye equations (first derived in 1929 by Debye for the case of dielectric relaxation) which can be found in detail in many textbooks and monographs (e.g. Zener 1948, Nowick and Berry 1972, Fantozzi 2001). The Debye equations can be written in different ways, e.g.

[1] This specific use of the alone-standing symbol Δ for the relaxation strength, following the common practice in the literature on anelastic relaxation, should not be confused with its general meaning as a difference sign in combinations like ΔW.

[2] Sometimes the loss angle ϕ is defined as "internal friction" (Nowick and Berry 1972, Fantozzi 2001), implying that internal friction would exist only in linear viscoelastic materials. Since there is no physical reason for such a restriction, we prefer the more general use of this term introduced earlier.

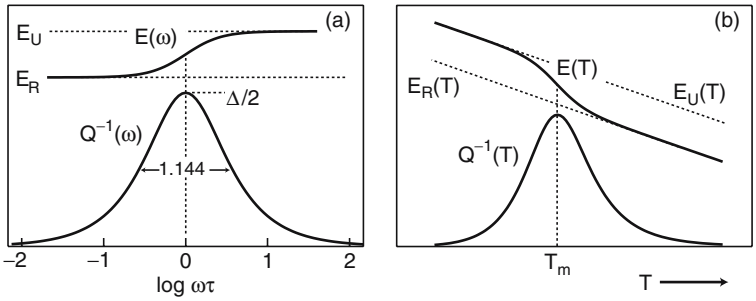

Fig. 1.3. Dynamic modulus E and internal friction Q^{-1} of the standard anelastic solid: (**a**) as a function of frequency on a log $\omega\tau$ scale; (**b**) as a function of temperature at constant frequency. In the latter case, the relaxation-induced step in $E(T)$ is superimposed on the intrinsic temperature dependence of $E_{\mathrm{U}}(T)$ and $E_{\mathrm{R}}(T)$

$$E'(\omega) = E_{\mathrm{R}}\left(1 + \Delta\frac{\omega^2{\tau_\varepsilon}^2}{1+\omega^2{\tau_\varepsilon}^2}\right) = E_{\mathrm{U}}\left(1 - \frac{\Delta}{1+\Delta}\frac{1}{1+\omega^2{\tau_\varepsilon}^2}\right) \tag{1.5}$$

and

$$Q^{-1}(\omega) = \frac{\Delta}{\sqrt{1+\Delta}}\frac{\omega\sqrt{\tau_\sigma\tau_\varepsilon}}{1+\omega^2\tau_\sigma\tau_\varepsilon}, \tag{1.6}$$

where E_{U}, E_{R}, Δ, τ_σ and τ_ε have the same meaning as in the quasi-static case considered above. In the case of $\Delta \ll 1$, these equations simplify to

$$E(\omega) = E'(\omega) = E_{\mathrm{R}}\left(1 + \Delta\frac{\omega^2\tau^2}{1+\omega^2\tau^2}\right) = E_{\mathrm{U}}\left(1 - \frac{\Delta}{1+\omega^2\tau^2}\right) \tag{1.7}$$

and

$$Q^{-1}(\omega) = \Delta\frac{\omega\tau}{1+\omega^2\tau^2}. \tag{1.8}$$

The resulting *Debye peak* $Q^{-1}(\omega)$, as shown in Fig. 1.3a, is characterised by a well-defined shape and width (1.144 at half-maximum on a $\log_{10}\omega\tau$ scale) with a damping maximum ${Q_{\mathrm{m}}}^{-1} = \Delta/2$ at $\omega\tau = 1$. The asymptotic behaviour for $\omega\tau \to 0$ and $\omega\tau \to \infty$ implies that at these limits the loss angle ϕ vanishes and the elliptic stress–strain hysteresis loop degenerates to a straight line (purely elastic behaviour with slopes E_{U} for $\omega\tau \gg 1$ and E_{R} for $\omega\tau \ll 1$), so that losses are detectable only in a certain range around $\omega\tau = 1$ ("*dynamic*" hysteresis).

1.4 Thermal Activation

Most of the known mechanisms of anelastic relaxation, to be described later in Chap. 2, have their origin in the thermally activated motion of various kinds of defects. In this case, a reciprocal Arrhenius equation

$$\tau = \tau_0 \exp\,(H/kT) \tag{1.9}$$

can be assumed for the relaxation time which now represents a reciprocal jump frequency of the defects ($\tau = \nu^{-1}$) to overcome the energy barrier H at the temperature T. Inserting (1.9) into (1.8), the Debye peak is now obtained also as a function of temperature at constant oscillation frequency $f = \omega/2\pi$ (Fig. 1.3b),

$$Q^{-1}(T) = \frac{\Delta}{2}\ \mathrm{sech}\ \frac{H}{k}\left(\frac{1}{T} - \frac{1}{T_m}\right), \tag{1.10}$$

where the peak (or maximum) temperature T_m is defined by the condition $\omega\tau = 1$, and sech $x = (\cosh\, x)^{-1} = 2/(\mathrm{e}^x + \mathrm{e}^{-x})$. On the reciprocal temperature scale (not shown in Fig. 1.3) the Debye peak is symmetric with a half-width of $2.635\,k/H$. The thermal activation parameters of the relaxation process, i.e., the (effective) activation enthalpy ("apparent activation energy") H and the "limit relaxation time" (reciprocal "attempt frequency")[3] $\tau_0 = {\nu_0}^{-1}$, are usually determined from the shift of the peak temperature T_m when changing the vibration frequency f, according to

$$\ln\left(\frac{f_2}{f_1}\right) = \frac{H}{k}\left(\frac{1}{T_{\mathrm{m}1}} - \frac{1}{T_{\mathrm{m}2}}\right). \tag{1.11}$$

This is even possible for loss peaks which are much broader than a Debye peak, which means that the underlying physical process includes a whole spectrum instead of a single value of relaxation times; in that case, *average* activation parameters are obtained (for more details on the analysis of relaxation spectra and peak deconvolution, see Nowick and Berry 1972, San Juan 2001). In fact, more or less broadened relaxation peaks are the experimental rule rather than the exception, so that most data on H and τ_0 given in this book, usually determined empirically from the frequency shift of T_m after (1.11), are in this sense some average values.

From this latter, experimental viewpoint, it is necessary to point out that the separation of H and τ_0, important for clarifying the relaxation mechanisms as well as for predicting the peak position at arbitrary frequencies, is inevitably connected with a loss in precision compared to directly measured data like T_m. A reliable evaluation of H and τ_0 – and even more of discrete or continuous spectra in these quantities – is highly sensitive to the quality of the experiments, and mainly requires the variation of frequency over a range as broad as possible. Such evaluated activation parameters may therefore be questionable in cases of scatter in the primary data or too small frequency variation, which can only partially be estimated from the information given in the tables of Chaps. 4 and 5. Since it has not been possible in this book to classify the quality of the literature data accordingly, the reader should be

[3] Sometimes the symbol τ_∞ (indicating the limit $T \to \infty$) is used instead of τ_0. On the other hand, the use of τ_0 is consistent with other common quantities like D_0 in the related diffusion equation $D = D_0 \exp(-H/kT)$.

aware that there may be strong variations especially in the reliability of the activation parameters H and τ_0. If doubts remain even after consulting the original papers, it is recommended to use the primary experimental data like T_m rather than H and τ_0.

1.5 Other Types of Internal Friction

Although the data collections in this book are focussed on anelastic relaxation, the main characteristics of other types of internal friction should also be considered briefly. It is useful to know about these characteristics not only for separating anelastic and other contributions when superimposed on each other, but also from the viewpoint of understanding the anelastic relaxation phenomena and mechanisms themselves.

Viscous damping, in the sense of non-recoverable linear viscoelasticity introduced earlier, can appear in quite different forms depending on the loading conditions and quantities considered. In contrast to anelasticity, all "relaxed" quantities are now either zero or infinite, and some parameters like Δ or τ_σ are meaningless; on the other hand, stress relaxation and the modulus-type response functions are quite analogous in both cases. For the Maxwell model as the simplest case, the dynamic functions $E'(\omega)$ and $E''(\omega)$ have the same form as for the standard anelastic solid, e.g. a "Debye peak" in $E''(\omega)$ with relaxation time τ_ε and peak height $E_\mathrm{U}/2$; however, the related loss tangent $\tan\,\phi = (\omega\tau_\varepsilon)^{-1}$ does not show any peak but goes to infinity in the low-frequency or high-temperature limit. An example of such viscous damping is the so-called "α relaxation" of metallic glasses (see Sect. 2.6.1).

Non-linear damping, i.e., internal friction beyond linear viscoelasticity, can be described by mechanical models containing specialised non-linear elements (Palmov 1998, Fantozzi 2001) in addition to springs and dashpots; such models are beyond the scope of this introduction, however. Generally, non-linearity always means that the loss factor becomes *amplitude-dependent*, whereas in linear viscoelasticity the related quantities in (1.4) do not depend on the amplitude of a sinusoidal vibration.

The amplitude dependence is usually connected with a "static" hysteresis component, i.e., a virtually frequency-independent contribution to the stress–strain hysteresis loop which does not vanish in the limit $\omega \to 0$. In simplified terms, such idealised type of non-linear, amplitude-dependent and frequency-independent behaviour is often named "hysteretic", as opposed to "relaxation" (i.e., linear, amplitude-independent and frequency-dependent); although in certain cases of non-linear relaxation this may be an oversimplification. For high-damping applications, "hysteretic" damping is generally preferred over relaxation because of its weak frequency dependence.

In contrast to linear viscoelasticity with always elliptically-shaped dynamic hysteresis loops (cf. (1.2)), non-linear damping may be based on many different

types and shapes of static hysteresis loops (see De Batist 2001 for some examples); the underlying mechanical behaviour may be of microplastic, pseudoelastic or other type depending on the related microscopic mechanisms. Since $\tan \phi$ is not well defined in these cases, non-linear internal friction should be expressed using more general definitions like the specific damping capacity Ψ in (1.1).

A few aspects of amplitude-dependent internal friction (ADIF) are addressed later in Chaps. 3.3–3.5. However, in spite of its importance for high-damping materials, ADIF is generally not included in the data collections of this book, with very few exceptions. A main reason – besides the mere quantity of data which would by far exceed the volume of the book – is that the amplitude dependence can be very sensitive to the microstructural state of the sample. This makes it more difficult to collect sufficiently detailed information to compare different ADIF studies to each other, but also to condense this information, if available, in the form of tables.

1.6 Measurement of Internal Friction

With ascending frequency, the experimental techniques of mechanical spectroscopy are generally divided into four groups: quasi-static, subresonance, resonance and wave-propagation (pulse-echo) methods. While measuring different quantities and response functions, they all can be used to determine internal friction of metallic materials, preferably under vacuum to avoid unwanted aerodynamic losses. More details about the following techniques, which can be mentioned only very briefly in this introduction, can be found in the books by Nowick and Berry (1972), Lakes (1999), Schaller et al. (2001), and related references.

Quasi-static tests can be performed using conventional mechanical testing equipment in two different ways: (1) in a quasi-static relaxation experiment (as creep/elastic after-effect $\varepsilon(t)$ at constant stress like in Fig. 1.2, or as stress relaxation $\sigma(t)$ at constant strain), or (2) in a cyclic measurement of the stress–strain hysteresis $\sigma(\varepsilon)$, e.g. at an alternating constant strain rate $\pm \mathrm{d}\varepsilon/\mathrm{d}t$.

The relaxation experiment (1) is suitable to study linear relaxation processes if the loading or unloading time of the testing machine is small compared to the relaxation time of interest. Measured are quasi-static response functions including quantities like Δ and τ, from which dynamic properties like internal friction can be calculated (Nowick and Berry 1972; cf. (1.8)). On the contrary, the cyclic test (2) is useful for obtaining the frequency-independent component of ADIF directly from (1.1) using the directly measured area ΔW of the "static" hysteresis loop.

Whereas quasi-static hysteresis can in principle be measured with arbitrary time functions of stress and strain, the remaining three *dynamic* methods ideally work with sinusoidal (harmonic) vibrations or waves with a well-defined frequency $\omega = 2\pi f$ and a wavelength λ for the related elastic waves. They

can be distinguished by means of the relation between λ and the length l of the sample.

Subresonant experiments, with $\lambda \gg l$ and no external inertia attached to the sample, are working in forced vibration far below the resonance frequency of the system. The directly measured quantity is the phase lag (loss angle) ϕ between stress and strain, from which internal friction is determined according to (1.4). Commercial instruments of this type ("dynamic mechanical analyser"), mostly working in bending mode, are widely used for polymers with a generally higher viscoelastic damping level. For metals, the low-frequency *forced torsion pendulum* is generally preferred because of its higher sensitivity. The main advantage of this technique is the possibility to perform isothermal experiments in a very large and continuous frequency range (10^{-4} to almost 10^2 Hz), which may be important in case of temperature-dependent structural changes (Rivière 2001b).

Resonant experiments form the largest and oldest group of mechanical spectroscopy methods, with the greatest variety of special techniques, and may be divided into subgroups where resonance either refers to the eigenvibrations of the sample ($\lambda \approx l$) or to a larger system ($\lambda \gg l$, with an external inertia attached to the sample). The most important resonance techniques – *torsion pendulum*, *vibrating-reed* (bending vibration of flat samples), *composite oscillator* (longitudinal vibration of rods), and *resonant ultrasound spectroscopy* of rectangular parallelepiped samples (Leisure 2004) – altogether span a frequency range from about 10^{-1} to more than 10^6 Hz.

Internal friction can be determined from resonant experiments in different ways. One possibility is the direct determination of ΔW and W by a careful analysis of the relative magnitudes of the input and output signals of the stationary resonant vibration which, however, needs a high stabilisation and calibration effort. More widely used are two other methods, called "resonant bandwidth" and "free decay", respectively. In the first case, the width of the resonance peak at the resonance frequency ω_r is measured using forced vibrations with constant excitation. If ω_1 and ω_2 denote the frequencies on both sides of the peak where the oscillation amplitude falls to $1/\sqrt{2}$ of its maximum value ("half-power" or "3 dB" points), the internal friction is given by[4]

$$Q^{-1} = (\omega_2 - \omega_1)/\omega_r. \tag{1.12}$$

[4] In fact, (1.1) and (1.12) are both found in the literature as definitions of the quality factor Q. In special cases of electrical circuits from which the concept of the quality factor is adopted, both expressions have been shown to be equivalent; possible differences at higher damping are less important for electrical networks which are normally designed for low damping. The related *mechanical* problem was analysed by Graesser and Wong (1992), using a linear "complex spring" model with frequency-independent loss factor. In this case agreement within 1% is found between both definitions for $Q^{-1} < 0.28$, whereas beyond that range the deviations grow rapidly up to a limit of $Q^{-1} = \sqrt{2}$ at $\tan\phi = 1$, above which Q^{-1} after (1.12) is no longer defined. Hence, if Q^{-1} is used for high damping values, the chosen definition should be indicated clearly.

The second, perhaps still most widely spread method uses free damped vibrations after turning off the excitation. The measured quantity is the logarithmic decrement δ defined as

$$\delta = \ln(A_n/A_{n+1}), \tag{1.13}$$

where A_n and A_{n+1} are the vibration amplitudes in two successive cycles. There are different ways of determining δ depending on the damping level of the sample, the quality of the signal, and details of measurement technique and data processing. Internal friction is usually determined by

$$Q^{-1} = \delta/\pi \tag{1.14}$$

as a well-known low-damping approximation. The deviations at high damping depend again on the exact response of the material; related results from the literature are restricted to special cases (sometimes also questionable) and will not be given here. In the perhaps most careful analysis available, Graesser and Wong (1992) give $Q^{-1} < 0.2$ as range of validity, within 1% deviation, for (1.14) in case of the "complex spring" model.

In *wave-propagation experiments*, short high-frequency pulses ($\lambda \ll l$; frequency about 10^6–10^9 Hz or even more) are sent through the sample. The attenuation coefficient

$$\alpha = -\mathrm{d}(\ln\ u(x))/\mathrm{d}x = \delta/\lambda, \tag{1.15}$$

where $u(x)$ is the envelope of the wave during propagation in x direction, corresponds to the logarithmic decrement δ that would be expected for a related free vibration. Hence, the internal friction is

$$Q^{-1} = \delta/\pi = \alpha\lambda/\pi \tag{1.16}$$

with limitations analogous to those mentioned earlier for (1.14).

In addition to these experimental standard methods, there are also some highly specialised, combined techniques like acoustic coupling or scanning local acceleration microscopy (Gremaud et al. 2001a,b). Furthermore, advanced microfabrication technology and the development of micro- or nanoelectromechanical systems (MEMS/NEMS) open new applications for classical resonance techniques using miniaturised resonators (Yasumura et al. 2000) or thin films on specially designed, complex-shaped oscillators (Liu and Pohl 1998, Harms et al. 1999).

http://www.springer.com/978-3-540-68757-3

Internal Friction in Metallic Materials
A Handbook
Blanter, M.S.; Golovin, I.S.; Neuhäuser, H.; Sinning, H.-R.
2007, XVII, 542 p., Hardcover
ISBN: 978-3-540-68757-3